

Effect of low concentrations of SiO₂ nanoparticles on the physical and chemical properties of sodium alginate-based films

Luís Marangoni Júnior^{a,b,*}, Renan Garcia da Silva^{a,c}, Carlos Alberto Rodrigues Anjos^b, Roniérik Pioli Vieira^c, Rosa Maria Vercelino Alves^a

^a Packaging Technology Center, Institute of Food Technology, Campinas, São Paulo, Brazil

^b Department of Food Engineering and Technology, School of Food Engineering, University of Campinas, Campinas, São Paulo, Brazil

^c Department of Bioprocess and Materials Engineering, School of Chemical Engineering, University of Campinas, Campinas, São Paulo, Brazil

ARTICLE INFO

Keywords:

Bio-based film
Nanocomposite
Food packaging
Thermal stability

ABSTRACT

This work investigated the effect of adding low concentrations of nano-SiO₂ (0.5, 1.0 and 1.5%) in the properties of films based on sodium alginate, to identify lower thresholds in the proportion of the reinforcing agent. It was found that, even in the smallest proportion, thermal stability of the nanocomposites improved significantly (with degradation onset increased by almost 15% compared with the control film). The surface morphology showed pronounced roughness at nano-SiO₂ concentrations greater than 1.0%, indicating agglomeration of part of the nanomaterial. Mechanical properties were reduced for the samples with concentrations equal to 1.0 and 1.5%, however, without significant differences between them. Conversely, water vapor and light barrier properties have not undergone significant changes in any formulation. Therefore, the use of 0.5% nano-SiO₂ in alginate films would be an easy and economically interesting way to improve thermal stability, without significantly reducing mechanical properties of the pure material.

1. Introduction

It is well-known petroleum-based plastics are the most commonly employed materials for food packaging (Marangoni et al., 2020). As much as these plastics are consolidated, numerous environmental aspects and consumer demand for safe and non-harmful materials make this theme of wide relevance for current and future research (Sharma et al., 2020). Polymers from biological sources (e.g. proteins and carbohydrates) stand out as important renewable and biodegradable raw materials (Marangoni Júnior et al., 2021). In this context, a considerable number of alternative biological sources demonstrate potential, but still need to be explored extensively to enable an appropriate relationship between performance and production cost.

Seaweed is abundant in the oceans, being a source of polysaccharides, proteins, peptides, lipids, amino acids, polyphenols and mineral salts (Brown et al., 2014). They can be classified into three main groups: brown algae (*Phaeophyceae*), green algae (*Chlorophyceae*) and red algae (*Rhodophyceae*) (Xu et al., 2017). In particular, brown algae are sources of alginates, one of the most versatile polysaccharides found in nature (Rahmani et al., 2017). The fact that it is a biodegradable and

non-toxic polymer to the human organism has expanded its applications in the pharmaceutical (Uyen et al., 2020), medical (Venkatesan et al., 2015), and food areas (Gheorghita Puscaselu et al., 2020).

One of the prominent applications of alginate has been in the production of films for food packaging (Senturk Parreidt et al., 2018). However, the fragility, high sensitivity to water, low thermal stability and low gas barrier properties, restrict such applications (Hou et al., 2019). Thus, obtaining nanocomposites using this biopolymer and nanometric scale materials as reinforcing agents has become an efficient and low-cost strategy for improving the overall properties of the films. Nanosilica (nano-SiO₂), for example, is an amorphous material with three-dimensional structure on a nanoscale (Hassannia-Kolae et al., 2016). Due to its excellent cost-benefit ratio, nanosilica has been extensively studied for this purpose (Fabbri et al., 2006; Kavya et al., 2013; Salimi et al., 2017; Tabatabaei et al., 2018; Yang et al., 2016).

Alginate-based films (pure or blended with other polymers) reinforced with nano-SiO₂ have been reported with great success in improving mechanical and thermal properties (Hou et al., 2019; Yang et al., 2016; Yang et al., 2018; Yang & Xia, 2017). Yang and Xia obtained alginate films containing nano-SiO₂ with concentrations between 1.5

* Corresponding author at: Rua Monteiro Lobato, 80 Cidade Universitária Zeferino Vaz, CEP: 13083-862 Campinas, SP, Brazil.

E-mail address: marangoni.junior@hotmail.com (L. Marangoni Júnior).

and 10%. Tensile strength and elongation at break were higher for nano-SiO₂ levels of approximately 4.5%. The films moisture content and water vapor barrier decreased due to the increase in nano-SiO₂ levels, but thermal stability improved in all cases (Yang & Xia, 2017). Although these values indicate improvements in most properties, roughness in surface morphology was observed due to possible nanomaterial agglomeration (Hou et al., 2019; Yang et al., 2018), which may be an indication of excess of this component. In this context, to what extent could the use of lower concentrations of nano-SiO₂ contribute to improving the properties of films?

The fundamental hypothesis of this study was that the reduction of the nano-SiO₂ levels would allow a greater dispersion along the alginate matrix and, even in low concentration it could enable the improvement of some properties of the resulting films. This fact would be relevant in the case of industrial production, as it would allow significant savings in resources and ease of processing the material. Therefore, the objective of this work is to evaluate the effect of low concentrations (0.5 to 1.5%) of nano-SiO₂ on the physical, chemical and morphological properties of alginate-based films. To the best of our knowledge, this is the first time this concentration threshold is explored for alginate/SiO₂ films, which could contribute to the understanding of the relationships between structure and properties, as to optimize the process.

2. Material and methods

2.1. Material

The materials used in the preparation of the films were: sodium alginate (SA) (CAS 905-38-3, purity of 99% viscosity (2% solution at 25 °C): 2.000 cps) (Dinâmica Química Contemporânea Ltda., Indaiatuba/SP, Brazil). It was reported in the literature that the SA used in this study has a molecular weight of 134,000 Da and ratio of guluronic (G) to mannuronic (M) acid groups (G/M) of 0.96 (Moreira Filho et al., 2020). Glycerol (Dinâmica Química Contemporânea Ltda., Indaiatuba/SP, Brazil), silica nanoparticles (nano-SiO₂) with an average particle size of 12 nm (Evonik/Degussa Brasil Ltda., Americana/SP, Brazil) and distilled water.

2.2. Preparation of the films

The casting method was adapted from Priyadarshi et al. (2021), and employed in the manufacture of sodium alginate/SiO₂ nanocomposite films. First, sodium alginate solutions (3% w/w) were prepared by dissolving the biopolymer in distilled water containing glycerol as a plasticizer (30% w/w, considering the mass of sodium alginate), and adding different concentrations of nano-SiO₂ (0.5, 1.0 and 1.5% w/w, considering the mass of sodium alginate). The solution was heated under stirring up to 80 °C. After reaching this temperature, the stirring continued for 20 min, to ensure a better solution homogeneity. Then, the final solution was treated in an ultrasound bath for 15 min, to ensure a homogeneous solution and elimination of bubbles. After this stage, 40 g of film-forming solutions were poured into polystyrene Petri dishes (140 mm diameter) and stabilized/dried at 40 °C for 20 h in a forced air circulation oven (Ethik Technology, Vargem Grande Paulista/SP, Brazil). Finally, after removing the films from the plates, they were conditioned, in an air-conditioned chamber (Weiss Technik, Reiskirchen, Germany) at 25 °C and 75% RH, as a step prior to the characterization processes. The films were identified as: SA, SA/0.5%SiO₂, SA/1.0%SiO₂ and SA/1.5%SiO₂.

2.3. Characterization of films

2.3.1. Film morphology

Film's surface and cross section were analyzed using scanning electron microscopy (SEM) (Leo 440i, LEO Electron Microscopy/Oxford, Cambridge, England). The samples were previously fractured with

liquid nitrogen, then fixed in metallic support with the aid of double-sided carbon tape and covered with gold in a sputter coater (SC7620, VG Microtech, Kent, United Kingdom). The visualization was performed with 1000× magnification, with a voltage of 15 kV and a current of 50 pA.

2.3.2. FT-IR spectroscopy

FT-IR analysis was performed using a Thermo Scientific spectrometer (Nicolet Continuum, Madison, USA). For nano-SiO₂, it was used the transmittance mode employing the accessory SBAP-IN BASEPLATE (KBr mode) at 4000–400 cm⁻¹, with a resolution of 4 cm⁻¹; for all nano-composite films it was used the attenuated total reflectance module (ATR), at 4000–650 cm⁻¹, with a resolution of 4 cm⁻¹.

2.3.3. Thermogravimetric analysis (TGA)

Thermal stability was determined using a Mettler Toledo Thermogravimetric Analyzer (TGA), model TGA/DSC1 (Schwerzenbach, Switzerland). The samples (10 mg) were heated from 25 to 600°, at a heating rate of 20 °C min⁻¹; and an N₂ flow of 50 ml min⁻¹.

2.3.4. X-ray diffraction (XRD)

X-ray diffraction was recorded in an X-ray analyzer (X'Pert-MPD, Philips, Almelo, Netherlands). The XRD measurements of pure nano-SiO₂, of the sodium alginate control film, as well as sodium alginate films with nano-SiO₂ were operated with Cu Kα radiation (λ = 1.54056 Å) at a scan rate of 0.033333°/s (step = 0.04° and time per step = 1.2 s), with the accelerated voltage of 40 kV and the applied current of 40 mA, ranging from 5 to 60°.

2.3.5. Film thickness

Thickness of the sodium alginate films were determined in a measurement system composed of a flat granite base and comparator clock (Mitutoyo Co., Kawasaki-Shi, Japan), with 0.1 μm resolution, after conditioning, for 48 h, at 25 ± 2 °C and 75 ± 5% RH. Measurements were performed using five random points from five specimens per formulation sample, in accordance with the standard ISO-4593 (1993).

2.3.6. Mechanical properties

The samples were cut with a width of 15 mm in a high precision equipment (RDS-100-C, ChemInstruments, OH, USA). Then, they were conditioned, for 48 h, at 25 ± 2 °C and 75 ± 5% RH. Tensile strength (MPa), elongation at break (%) and modulus of elasticity (MPa) were determined following ASTM-D882 (2018), using a universal testing machine (Instron, 5966-E2, Norwood, USA). The tests were carried out with a 100 N load cell, with a speed of 12 mm min⁻¹ and with initial grip separation of 50 mm. Five repetitions were carried out for each sample.

2.3.7. Moisture content

Moisture content (MC) of the films was obtained by gravimetry, after drying at 105 °C for 24 h, in an oven (Ethik Technology, Vargem Grande Paulista/SP, Brazil), using an analytical balance (Mettler Toledo, Columbus, Ohio, USA) 10⁻⁴ g resolution. The values of the MC (%) were determined, in four repetitions, for each sample analyzed, according to Eq. (1):

$$MC = \frac{w_i - w_f}{w_i} \times 100\% \quad (1)$$

in which w_i and w_f are the initial and final weights of the sample, respectively.

2.3.8. Water vapor permeability

The water vapor transmission rates (WVTR) were determined using the gravimetric method of analysis, based on the ASTM-E96/E96M (2016). Capsules with a permeation area of 50 cm², using an analytical balance (Mettler Toledo, Columbus, Ohio, USA) resolution of 10⁻⁴ g. The tests were carried out at 25 °C and 75% RH in an air-conditioned

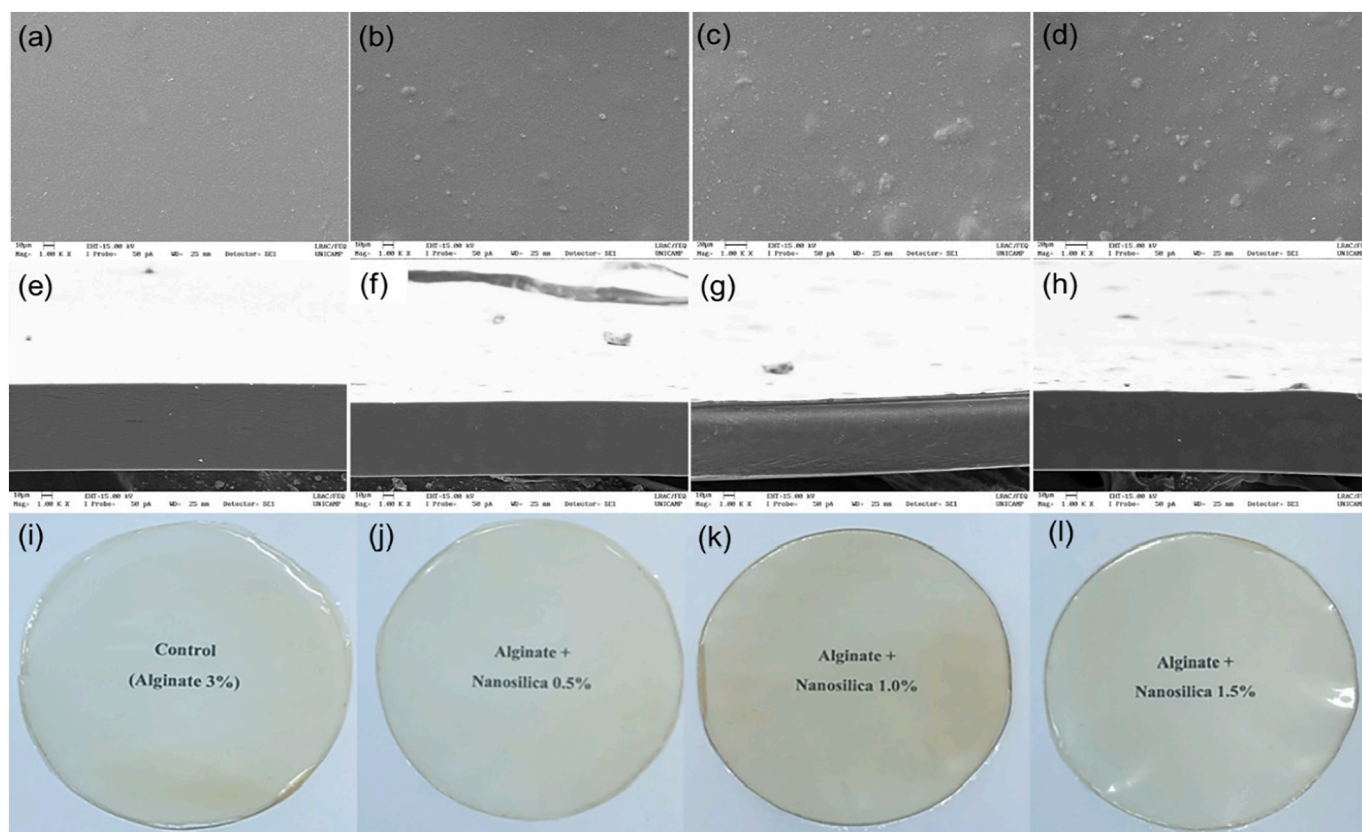


Fig. 1. SEM images of the surface, cross section and photographs of the sodium alginate films with nano-SiO₂. (a), (e) and (i) SA; (b), (f) and (j) SA/0.5%SiO₂; (c), (g) and (k) SA/1.0%SiO₂; (d), (h) and (l) SA/1.5%SiO₂.

chamber (Weiss Technik, Reiskirchen, Germany), with anhydrous calcium chloride desiccant. The WVTR ($\text{g m}^{-2} \text{day}^{-1}$) were determined from the slope of the function “change in weight vs. time”, and the WVP ($\text{g m}^{-1} \text{s}^{-1} \text{Pa}^{-1}$) of the films were calculated according to Eq. (2):

$$WVP = \frac{WVTR \times e}{p_s \times RH_1} \quad (2)$$

In which e is the specimen average thickness (μm), p_s is the water vapor saturation pressure (23.756 mmHg at 25 °C), RH_1 is the relative humidity of the chamber (75% = factor 0.75), since the relative humidity inside the capsule is considered to be zero.

2.3.9. Light transmission

Light transmission was determined in triplicate using a double-beam UV–visible spectrophotometer (Analytik Jena - Specord 210) using an integrating sphere, with a scanning speed of 120 nm min^{-1} and a scanning range of 200 to 800 nm, according to ASTM-E-1348 (2015).

2.3.10. Statistical analysis

The results were statistically evaluated by means of analysis of variance (ANOVA) and the Tukey test to compare the averages ($p < 0.05$).

3. Results and discussions

3.1. Film morphology and chemical structure

The surfaces and cross sections morphology of the nanocomposite films were examined using a scanning electron microscope (with magnification of 1000 \times) and also by photographs (Fig. 1). It was verified that the surfaces of all samples did not present empty spaces or cracks. The control sample (films without nano-SiO₂) showed a smooth

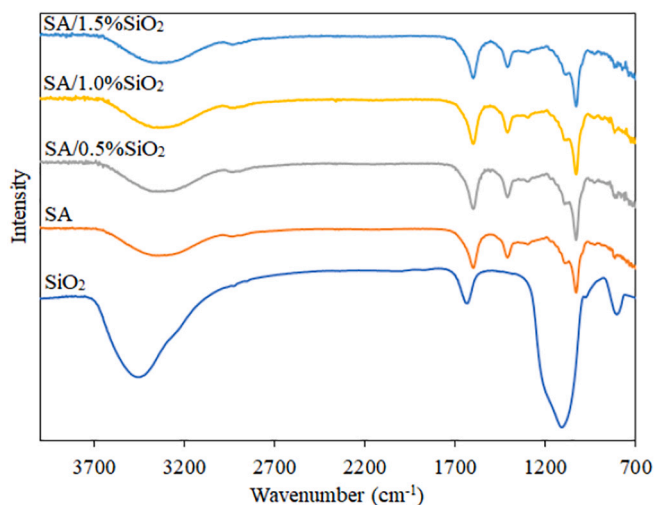


Fig. 2. FT-IR spectra for nano-SiO₂, pure sodium alginate (SA) and alginate-based films added with 0.5; 1.0 and 1.5% nano-SiO₂.

and homogeneous appearance (Fig. 1(a)). However, the surface of the other films, even with low concentrations of nano-SiO₂, had a rough appearance, and this character was accentuated as the proportion of nano-SiO₂ increased from 0.5 to 1.5% (Fig. 1(b)–(d)). Through Fig. 1(d), it can be seen that, for the concentration of nano-SiO₂ equal to 1.5%, a significant part of the particles was agglomerated in domains larger than 1 μm , suggesting difficulty in exfoliating the material along the matrix.

SEM images of the film cross sections are shown in Fig. 1(e)–(h). A uniform and smooth appearance was observed in all samples, suggesting

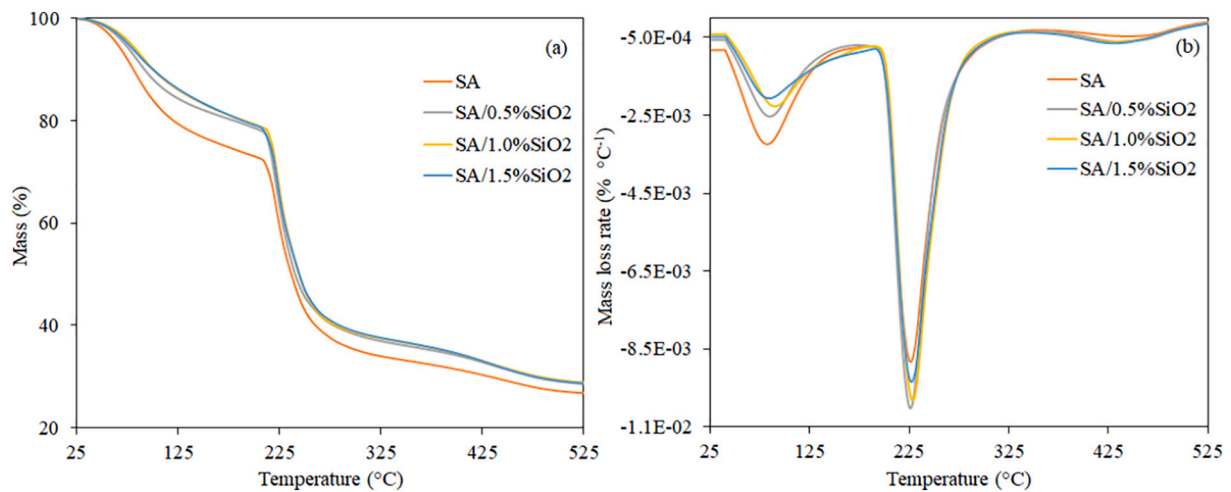


Fig. 3. TGA (a) and DTG (b) curves of the sodium alginate-based films added with 0.5, 1.0 and 1.5% nano-SiO₂.

Table 1

Initial degradation (T_{onset}) and maximum decomposition (T_{max}) temperatures of the sodium alginate-based films added with 0.5, 1.0 and 1.5% nano-SiO₂.

Sample	1st thermal event			2nd thermal event		
	T_{onset}	T_{max}	Mass loss (%)	T_{onset}	T_{max}	Mass loss (%)
SA	52.41	81.81	15.40	213.60	225.89	73.55
SA/0.5% SiO ₂	56.31	83.95	11.75	212.05	224.78	71.82
SA/1.0% SiO ₂	60.99	88.95	11.54	214.61	226.62	71.69
SA/1.5% SiO ₂	54.26	83.43	11.23	214.05	226.13	71.84

a good dispersion of the material throughout the film matrix. These images contrast with what was observed in the surface morphology, indicating that part of the agglomerated nano-SiO₂ particles were deposited on the material surface during the preparation process. The photographs of all samples, Fig. 1(i)–(l), indicate that the addition of nano-SiO₂ in these concentration ranges did not present significant visual impacts on the material.

The FT-IR spectra of the sodium alginate films are shown in Fig. 2. The absorption bands characteristic of the SA film were found at approximately 3410 cm⁻¹, which may be due to the hydroxyl group (-OH) (Han et al., 2010; Pereira et al., 2011), at 1595 cm⁻¹ and 1410 cm⁻¹, corresponding to vibrations of asymmetric elongation of the C–O bond of the COO⁻ group (Alves et al., 2020; Costa et al., 2018; Pereira et al., 2011), at 1030 cm⁻¹ corresponding to the antisymmetric elongation of C–O–C (Alves et al., 2020; Lawrie et al., 2007) and at 820 cm⁻¹ characteristic peak of mannuronic acid residues (Alves et al., 2020; Fertah et al., 2017). The results of the nanocomposite sodium alginate films FT-IR spectra showed a similar pattern, confirming that no chemical bond was created after the addition of nano-SiO₂. Similar behavior was observed for PVA/xylan films added with nano-ZnO and nano-SiO₂ (Liu et al., 2019), and fish gelatin/carrageenan with nano-SiO₂ (Tabatabaei et al., 2018).

3.2. Thermal stability

Thermal degradation profiles of the sodium alginate/SiO₂ films are shown in Fig. 3. The results show that the incorporation of nano-SiO₂, even in low concentrations, resulted in an improvement in the stability of the SA films, which can be confirmed by mass loss events (Fig. 3(a) and Table 1). The degradation of all tested samples occurred mainly in two different thermal events. The first one starting at 52 °C for the

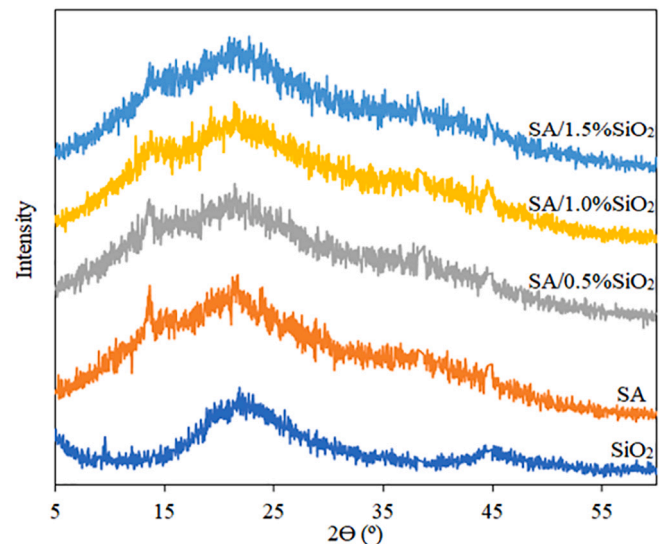


Fig. 4. XRD of nano-SiO₂, pure sodium alginate (SA) and alginate-based films added with 0.5, 1.0 and 1.5% nano-SiO₂.

control film and between 54 °C and 61 °C for the films containing 0.5, 1.0 and 1.5% nano-SiO₂. This event is associated with the evaporation of moisture present in the film. The maximum degradation of the samples occurred at a temperature of approximately 225 °C, with a loss of mass slightly higher only for the control sample. This maximum degradation refers to the breakdown of glycosidic bonds and the elimination of adjacent hydroxyl groups (Pongjanyakul et al., 2005; Soares et al., 2004; Yang et al., 2016). It is interesting to note that similar profiles have been obtained in the literature for much higher concentrations of nano-SiO₂ (Yang et al., 2016; Yang & Xia, 2017), suggesting that the low concentrations used in this study also contribute to the improvement of the film's thermal stability. The stages of mass loss can be better observed in the DTG curves (Fig. 3(b)).

3.3. X-ray diffraction

Fig. 4 illustrates the XRD spectra of the composite films. Pure nano-SiO₂ showed a broad and strong diffraction peak at $2\theta \approx 23^\circ$, indicating its amorphous structure. Similar results were obtained in other studies (Hou et al., 2019; Salimi et al., 2017; Wang et al., 2016). The XRD spectra of the control SA sample showed a small peak at $2\theta \approx 13^\circ$, and

Table 2
Thickness and mechanical properties of sodium alginate films with nano-SiO₂.

Sample	Thickness (μm)	Tensile Strength (MPa)	Elongation at Break (%)	Modulus of elasticity (MPa)
SA	89.1 ± 13.8 ^b	29.2 ± 3.9 ^a	29.1 ± 4.6 ^a	677.3 ± 128.0 ^a
SA/0.5% SiO ₂	100.9 ± 16.0 ^{ab}	30.6 ± 3.8 ^a	29.3 ± 2.6 ^a	809.6 ± 32.7 ^a
SA/1.0% SiO ₂	103.3 ± 15.9 ^a	21.1 ± 4.9 ^b	23.3 ± 3.5 ^{ab}	688.0 ± 90.4 ^a
SA/1.5% SiO ₂	106.4 ± 18.2 ^a	20.4 ± 4.3 ^b	20.0 ± 5.6 ^b	654.5 ± 199.2 ^a

The results are expressed as mean ± standard deviation.

^{a, b, c} The means, followed by the same letter, in the column, do not differ at the 95% confidence level ($p < 0.05$).

the higher de proportion of nano silica the lower the intensity of this peak. This result indicates the crystallinity of alginate was reduced by the addition of nano-SiO₂. It's important to mention that a broad diffraction peak at $2\theta \approx 20^\circ$ was also observed for all SA-based films, which was slightly different from some alginate-based films XRD profiles provided in the literature (Yang et al., 2016; Yang & Xia, 2017). This is frequent, since alginate is a natural polymer obtained by different sources of raw materials and the film preparations differ considerably, causing small changes in its morphology. Finally, there is no XRD profile of nanocomposites showed characteristic peaks of nano-SiO₂. This result can be attributed to the low concentration and also by an exfoliation of party of the nanomaterial throughout the film.

3.4. Thickness and mechanical properties

The average thicknesses for SA films are listed in Table 2. The results indicate that the addition of 0.5% nano-SiO₂ in the films did not result in a significant difference ($p < 0.05$) in the thickness in relation to the control film (SA). On the other hand, the thickness of the films was greater as the concentration of nano-SiO₂ increased (1.0 and 1.5%), from $89.1 \pm 13.8 \mu\text{m}$ to $103.3 \pm 15.9 \mu\text{m}$ and $106.4 \pm 18.2 \mu\text{m}$, respectively. Similar behavior was observed by Roy and Rhim (2020), for sodium alginate films added with CuS. These results are supported by the work of Yerramathi et al. (2021) & Rangel-Marrón et al. (2013), which state that the thickness is dependent on the concentrations of the film-forming components.

Tensile strength (TS), elongation at break (EB) and modulus of elasticity (ME) of the SA films are shown in Table 2. The addition of 0.5% nano-SiO₂ did not significantly influence ($p < 0.05$) the TS and EB of the SA films. However, SA films with concentrations of 1.0 and 1.5% nano-SiO₂ showed a significant reduction ($p < 0.05$) in TS and EB, from 29.2 MPa to 20.4 MPa, and 29.1% to 20.0%, respectively. Similar behavior was found by Roy and Rhim (2020) for sodium alginate films with CuS. This phenomenon indicated that the addition of low concentrations of nano-SiO₂ did not result in a reinforcing effect in the polymer matrix, different from the behavior observed by Hou et al. (2019) for agar/alginate films with higher concentrations of nano-SiO₂ (2.5–10.0%). In addition, the reduction in TS and EB can be attributed to the inadequate formation of intermolecular hydrogen bonds (Voon et al., 2012) and also as a result of the aggregation of nanoparticles (Hassannia-Kolaee et al., 2016; Li et al., 2011; Shahabi-Ghahfarrokhi et al., 2015), which corroborates the SEM images. Finally, the concentrations of nano-SiO₂ evaluated did not significantly influence the ME results of SA films.

3.5. Moisture content and water vapor permeability

Moisture content is measured to estimate the water-binding capacity of biopolymer-based films. Sodium alginate films showed high levels of

Table 3
Moisture content and water vapor permeability of sodium alginate films with nano-SiO₂.

Sample	Moisture content (%)	WVTR (g m ⁻² day ⁻¹)	WVP ($\times 10^{-10}$ g m ⁻¹ s ⁻¹ Pa ⁻¹)
SA	81.3 ± 0.3 ^b	906.3 ± 23.7 ^a	4.0 ± 0.4 ^a
SA/0.5% SiO ₂	79.8 ± 0.3 ^c	860.1 ± 54.5 ^a	4.2 ± 0.4 ^a
SA/1.0% SiO ₂	82.2 ± 0.3 ^a	767.9 ± 101.8 ^a	3.9 ± 0.4 ^a
SA/1.5% SiO ₂	82.2 ± 0.3 ^a	940.7 ± 81.3 ^a	5.0 ± 1.0 ^a

The results are expressed as mean ± standard deviation.

^{a, b, c} The means, followed by the same letter, in the column, do not differ at the 95% confidence level ($p < 0.05$).

moisture content, due to their high affinity with water, ranging from $79.8 \pm 0.3\%$ and $82.2 \pm 0.3\%$ (Table 3). These results are in line with the high values determined by Yerramathi et al. (2021) for edible sodium alginate films manufactured through the ferulic acid crosslinking mechanism. A significant reduction ($p < 0.05$) was observed in the humidity level of sodium alginate film with 0.5% nano-SiO₂ in relation to the control. In this case, greater interaction between hydroxyls of the nanomaterial and carboxylates of the biopolymer matrix could have contributed to the reduction of the moisture content. On the other hand, an opposite effect was observed in the films with the addition of 1.0 and 1.5% nano-SiO₂, that is, a significant increase ($p < 0.05$) in relation to the control, being another indicative result for possible agglomeration of part of the nano-SiO₂ at higher concentrations.

The WVTR and WVP of the nanocomposite films ranged from 940.7 ± 81.3 to 767.9 ± 101.8 (g m⁻² day⁻¹) and from 3.9 ± 0.4 to 5.0 ± 1.0 ($\times 10^{-10}$ g m⁻¹ s⁻¹ Pa⁻¹), respectively (Table 3). However, these values did not differ significantly from each other ($p < 0.05$). Although there was no significant difference in the water vapor permeability values, films with 1.0% nano-SiO₂ showed lower values of WVTR and WVP compared to the other films. However, it is possible to state that low concentrations of nano-SiO₂ (0.5–1.5%) were not sufficient to improve the water vapor barrier properties. These findings are mainly attributed to the agglomeration of part of the nanoparticles on the surface of the films, as observed in the SEM images. Similar results were observed for low concentrations (0.5–2.0%) of nano-CuS in agar films by Roy et al. (2019).

It was expected that there would be a decrease in the water vapor permeability of the films due to the increase in the length of the path for the diffusion of water vapor formed by the addition of nano-SiO₂ distributed in the polymeric matrix (Shankar et al., 2017). This phenomenon did not occur in the sodium alginate/nano-SiO₂ films and, probably, this event is justified by the low concentrations of nano-SiO₂ used in this study. However, it is important to note that the inclusion of a material (nano-SiO₂) with high intrinsic thermal stability, even in small concentrations, tends to increase the thermal stability of the film as a whole, as reported previously. The mechanisms of action in both properties are different. In the case of WVP, the concentrations of nano-SiO₂ added were not sufficient to increase the water vapor diffusion path. But these concentrations were sufficient to reinforce the polymer matrix against the thermal degradation process, as is already well known in the literature.

3.6. Light transmission

The transmittance of films applied to food packaging is an important parameter for various applications (Ramakrishnan et al., 2021). In general, the incidence of light in foods can trigger reactions of degradation of macro and micro molecules, such as oxidation and degradation of lipids, vitamins, and pigments (Marangoni Júnior, Vieira, & Anjos, 2020). Therefore, the packaging material applied to these foods must

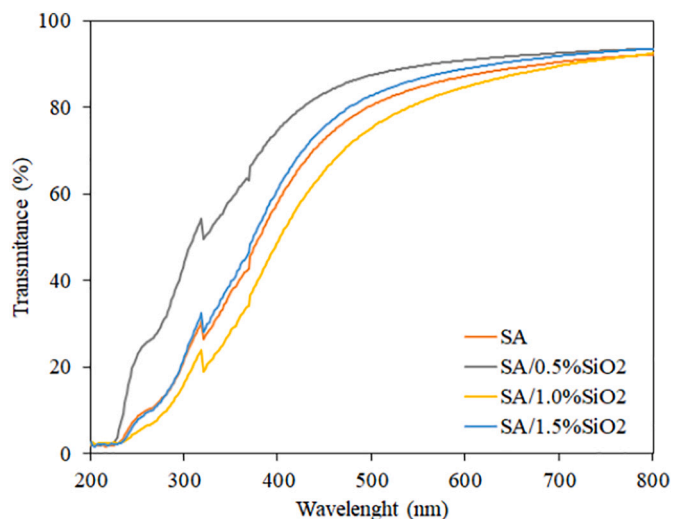


Fig. 5. Light transmission profile (%) of sodium alginate films with and without nano-SiO₂.

provide a light barrier to minimize these reactions (Marangoni Júnior, Alves, et al., 2020). The light transmission of sodium alginate films with and without nano-SiO₂ was measured in the 200–800 nm wavelength range (Fig. 5). The light transmission profile of the different evaluated films was similar, where the light transmission of the films in the UV range (200–400 nm) was <60%. However, for the visible range (400–800 nm) these films had a low light barrier, with transmittance ranging from 60% to 90%. In this context, the interaction between nano-SiO₂ and the molecules of the polymeric matrix of SA did not influence the absorption or reflection of UV and visible light. However, it is important to note that depending on the application of these films, transparency is desirable, as in the case of coatings and fruits and vegetables.

4. Conclusions

Inferior properties still remain a limiting factor for the use of sodium alginate-based films. In this sense, the use of nano-SiO₂ in the formulation of films becomes an effective strategy for a possible improvement in the material performance. However, in many cases, high concentrations of nano-SiO₂ can remarkably reduce the performance (e.g., reduction of film elongation), and also increase the production costs of biopolymer-bases films. In this context, this study investigated what would be the effects of low nano-SiO₂ loads as reinforcement in SA-based films. The results showed low concentrations of SiO₂ nanoparticles can be easily incorporated in sodium alginate-based films without significant changes in their most general properties. It was demonstrated that, the lower concentration of nano-SiO₂ (0.5%) evaluated significantly improved the thermal stability of the films without affecting the morphological, mechanical and barrier properties. Therefore, the use of low concentrations of nano-SiO₂ could represent an economical easy dissolution of nanoparticles strategy for the manufacture of alginate/SiO₂ nanocomposite, which would allow possible future applications as food packaging.

CRedit authorship contribution statement

Luís Marangoni Júnior: Conceptualization, Data curation, Formal analysis, Funding acquisition, Investigation, Methodology, Project administration, Resources, Writing – original draft, Writing – review & editing. **Renan Garcia da Silva:** Formal analysis, Investigation, Writing – review & editing. **Carlos Alberto Rodrigues Anjos:** Writing – review & editing. **Roniériki Pioli Vieira:** Conceptualization, Data curation,

Formal analysis, Funding acquisition, Investigation, Methodology, Project administration, Resources, Supervision, Writing – original draft, Writing – review & editing. **Rosa Maria Vercelino Alves:** Conceptualization, Data curation, Formal analysis, Funding acquisition, Investigation, Methodology, Project administration, Resources, Supervision, Writing – review & editing.

Declaration of competing interest

The authors declare no conflicts of interest.

Acknowledgments

The authors acknowledge the *Espaço da Escrita – Coordenadoria Geral da Universidade – UNICAMP* – for the language services provided, the National Council for Scientific and Technological Development (CNPq). This study was partly financed by the Coordination for the Improvement of Higher Education Personnel – Brazil (CAPES) – Financial Code 001.

References

- Alves, D., Cerqueira, M. A., Pastrana, L. M., & Sillankorva, S. (2020). Entrapment of a phage cocktail and cinnamaldehyde on sodium alginate emulsion-based films to fight food contamination by *Escherichia coli* and *Salmonella* Enteritidis. *Food Research International*, 128(October 2019), Article 108791. <https://doi.org/10.1016/j.foodres.2019.108791>
- ASTM-D882. (2018). *Standard test method for tensile properties of thin plastic sheeting*. West Conshohocken.
- ASTM-E-1348. (2015). *Standard test method for transmittance and color by spectrophotometry using hemispherical geometry*. West Conshohocken.
- ASTM-E96/E96M. (2016). *Standard test methods for water vapor transmission of materials*. West Conshohocken.
- Brown, E. M., Allsopp, P. J., Magee, P. J., Gill, C. I. R., Nitecki, S., Strain, C. R., & McSorley, E. M. (2014). Seaweed and human health. *Nutrition Reviews*, 72(3), 205–216. <https://doi.org/10.1111/nure.12091>
- Costa, M. J., Marques, A. M., Pastrana, L. M., Teixeira, J. A., Sillankorva, S. M., & Cerqueira, M. A. (2018). Physicochemical properties of alginate-based films: Effect of ionic crosslinking and mannuronic and guluronic acid ratio. *Food Hydrocolloids*, 81, 442–448. <https://doi.org/10.1016/j.foodhyd.2018.03.014>
- Fabbri, P., Singh, B., Leterrier, Y., Manson, J.-A. E., Messori, M., & Pilati, F. (2006). Cohesive and adhesive properties of polycaprolactone/silica hybrid coatings on poly (methyl methacrylate) substrates. *Surface and Coatings Technology*, 200(24), 6706–6712. <https://doi.org/10.1016/j.surfcoat.2005.10.003>
- Fertah, M., Belfkira, A., Dahmane, E. M., Taourirte, M., & Brouillette, F. (2017). Extraction and characterization of sodium alginate from Moroccan *Laminaria digitata* brown seaweed. *Arabian Journal of Chemistry*, 10, S3707–S3714. <https://doi.org/10.1016/j.arabj.2014.05.003>
- Gheorghita Puscaselu, R., Lobiuc, A., Dimian, M., & Covasa, M. (2020). Alginate: From food industry to biomedical applications and management of metabolic disorders. *Polymers*. <https://doi.org/10.3390/polym12102417>
- Han, J., Zhou, Z., Yin, R., Yang, D., & Nie, J. (2010). Alginate-chitosan/hydroxyapatite polyelectrolyte complex porous scaffolds: Preparation and characterization. *International Journal of Biological Macromolecules*, 46(2), 199–205. <https://doi.org/10.1016/j.ijbiomac.2009.11.004>
- Hassannia-Kolaee, M., Khodaiyan, F., Pourahmad, R., & Shahabi-Ghahfarrokhi, I. (2016). Development of ecofriendly bionanocomposite: Whey protein isolate/pullulan films with nano-SiO₂. *International Journal of Biological Macromolecules*, 86, 139–144. <https://doi.org/10.1016/j.ijbiomac.2016.01.032>
- Hou, X., Xue, Z., Xia, Y., Qin, Y., Zhang, G., Liu, H., & Li, K. (2019). Effect of SiO₂ nanoparticle on the physical and chemical properties of eco-friendly agar/sodium alginate nanocomposite film. *International Journal of Biological Macromolecules*, 125, 1289–1298. <https://doi.org/10.1016/j.ijbiomac.2018.09.109>
- ISO-4593. (1993). *Plastics: Film and sheeting determination of thickness by mechanical scanning*. Switzerland.
- Kavya, K. C., Jayakumar, R., Nair, S., & Chennazhi, K. P. (2013). Fabrication and characterization of chitosan/gelatin/nSiO₂ composite scaffold for bone tissue engineering. *International Journal of Biological Macromolecules*, 59, 255–263. <https://doi.org/10.1016/j.ijbiomac.2013.04.023>
- Lawrie, G., Keen, I., Drew, B., Chandler-Temple, A., Rintoul, L., Fredericks, P., & Grøndahl, L. (2007). Interactions between alginate and chitosan biopolymers characterized using FTIR and XPS. *Biomacromolecules*, 8(8), 2533–2541. <https://doi.org/10.1021/bm070014y>
- Li, Y., Jiang, Y., Liu, F., Ren, F., Zhao, G., & Leng, X. (2011). Fabrication and characterization of TiO₂/whey protein isolate nanocomposite film. *Food Hydrocolloids*, 25(5), 1098–1104. <https://doi.org/10.1016/j.foodhyd.2010.10.006>
- Liu, X., Chen, X., Ren, J., Chang, M., He, B., & Zhang, C. (2019). Effects of nano-ZnO and nano-SiO₂ particles on properties of PVA/xylan composite films. *International Journal of Biological Macromolecules*, 132, 978–986. <https://doi.org/10.1016/j.ijbiomac.2019.03.088>

- Marangoni Júnior, L., Alves, R. M. V., Moreira, C. Q., Cristianini, M., Padula, M., & Anjos, C. A. R. (2020). High-pressure processing effects on the barrier properties of flexible packaging materials. *Journal of Food Processing and Preservation*. <https://doi.org/10.1111/jfpp.14865>
- Marangoni Júnior, L., Vieira, R. P., & Anjos, C. A. R. (2020). Kefiran-based films: Fundamental concepts, formulation strategies and properties. *Carbohydrate Polymers*, 246(May), Article 116609. <https://doi.org/10.1016/j.carbpol.2020.116609>
- Marangoni Júnior, L., Vieira, R. P., Jamroz, E., & Anjos, C. A. R. (2021). Furcellaran: An innovative biopolymer in the production of films and coatings. *Carbohydrate Polymers*, 252, Article 117221. <https://doi.org/10.1016/j.carbpol.2020.117221>
- Marangoni, L., Fávoro Perez, M.Á., Torres, C. D., Cristianini, M., Massaharu Kiyataka, P. H., Albino, A. C., ... Rodrigues Anjos, C. A. (2020). Effect of high-pressure processing on the migration of ϵ -caprolactam from multilayer polyamide packaging in contact with food simulants. *Food Packaging and Shelf Life*, 26. <https://doi.org/10.1016/j.foodpsl.2020.100576>
- Moreira Filho, R. N. F., Vasconcelos, N. F., Andrade, F. K., Rosa, M. d. F., & Vieira, R. S. (2020). Papanin immobilized on alginate membrane for wound dressing application. *Colloids and Surfaces B: Biointerfaces*, 194(June), Article 111222. <https://doi.org/10.1016/j.colsurfb.2020.111222>
- Pereira, R., Tojeira, A., Vaz, D. C., Mendes, A., & Bártolo, P. (2011). Preparation and characterization of films based on alginate and aloe vera. *International Journal of Polymer Analysis and Characterization*, 16(7), 449–464. <https://doi.org/10.1080/1023666X.2011.599923>
- Pongjanyakul, T., Priprem, A., & Puttipipatkachorn, S. (2005). Investigation of novel alginate–magnesium aluminum silicate microcomposite films for modified-release tablets. *Journal of Controlled Release*, 107(2), 343–356. <https://doi.org/10.1016/j.jconrel.2005.07.003>
- Priyadarshi, R., Kim, H. J., & Rhim, J. W. (2021). Effect of sulfur nanoparticles on properties of alginate-based films for active food packaging applications. *Food Hydrocolloids*, 110(July 2020), Article 106155. <https://doi.org/10.1016/j.foodhyd.2020.106155>
- Rahmani, B., Hosseini, H., Khani, M., Farhoodi, M., Honarvar, Z., Feizollahi, E., ... Shojaee-Aliabadi, S. (2017). Development and characterisation of chitosan or alginate-coated low density polyethylene films containing *Satureja hortensis* extract. *International Journal of Biological Macromolecules*, 105, 121–130. <https://doi.org/10.1016/j.ijbiomac.2017.07.002>
- Ramakrishnan, R. K., Wacławek, S., Černík, M., & Padil, V. V. T. (2021). Biomacromolecule assembly based on gum kondagogu-sodium alginate composites and their expediency in flexible packaging films. *International Journal of Biological Macromolecules*, 177, 526–534. <https://doi.org/10.1016/j.ijbiomac.2021.02.156>
- Rangel-Marrón, M., Montalvo-Paquiní, C., Palou, E., & López-Malo, A. (2013). Optimization of the moisture content, thickness, water solubility and water vapor permeability of sodium alginate edible films. In *Recent advances in chemical engineering, biochemistry and computational chemistry optimization* (pp. 72–78).
- Roy, S., & Rhim, J. W. (2020). Effect of CuS reinforcement on the mechanical, water vapor barrier, UV-light barrier, and antibacterial properties of alginate-based composite films. *International Journal of Biological Macromolecules*, 164, 37–44. <https://doi.org/10.1016/j.ijbiomac.2020.07.092>
- Roy, S., Rhim, J. W., & Jaiswal, L. (2019). Bioactive agar-based functional composite film incorporated with copper sulfide nanoparticles. *Food Hydrocolloids*, 93(February), 156–166. <https://doi.org/10.1016/j.foodhyd.2019.02.034>
- Salimi, F., Tahmasobi, K., Karami, C., & Jahangiri, A. (2017). Preparation of modified nano-SiO₂ by bismuth and iron as a novel remover of methylene blue from water solution. *Journal of the Mexican Chemical Society*, 61(3), 250–259. <https://doi.org/10.29356/jmcs.v61i3.351>
- Senturk Parreidt, T., Müller, K., & Schmid, M. (2018). Alginate-based edible films and coatings for food packaging applications. *Foods*. <https://doi.org/10.3390/foods7100170>
- Shahabi-Ghahfarrokhi, I., Khodaiyan, F., & Mousavi, M. (2015). Preparation of UV-protective kefir/nano-ZnO nanocomposites: Physical and mechanical properties. *International Journal of Biological Macromolecules*, 72, 41–46. <https://doi.org/10.1016/j.ijbiomac.2014.07.047>
- Shankar, S., Wang, L. F., & Rhim, J. W. (2017). Preparation and properties of carbohydrate-based composite films incorporated with CuO nanoparticles. *Carbohydrate Polymers*, 169, 264–271. <https://doi.org/10.1016/j.carbpol.2017.04.025>
- Sharma, R., Jafari, S. M., & Sharma, S. (2020). Antimicrobial bio-nanocomposites and their potential applications in food packaging. *Food Control*, 112(January), Article 107086. <https://doi.org/10.1016/j.foodcont.2020.107086>
- Soares, J. P., Santos, J. E., Chierice, G. O., & Cavalheiro, E. T. G. (2004). Thermal behavior of alginate acid and its sodium salt. *Ecl\copyrightica Qu\~Mica*, 29, 57–64.
- Tabatabaei, R. H., Jafari, S. M., Mirzaei, H., Nafchi, A. M., & Dehnad, D. (2018). Preparation and characterization of nano-SiO₂ reinforced gelatin-k-carrageenan biocomposites. *International Journal of Biological Macromolecules*, 111, 1091–1099. <https://doi.org/10.1016/j.ijbiomac.2018.01.116>
- Uyen, N. T. T., Hamid, Z. A. A., Tram, N. X. T., & Ahmad, N. (2020). Fabrication of alginate microspheres for drug delivery: A review. *International Journal of Biological Macromolecules*, 153, 1035–1046. <https://doi.org/10.1016/j.ijbiomac.2019.10.233>
- Venkatesan, J., Bhatnagar, I., Manivasagan, P., Kang, K.-H., & Kim, S.-K. (2015). Alginate composites for bone tissue engineering: A review. *International Journal of Biological Macromolecules*, 72, 269–281. <https://doi.org/10.1016/j.ijbiomac.2014.07.008>
- Voon, H. C., Bhat, R., Easa, A. M., Liong, M. T., & Karim, A. A. (2012). Effect of addition of halloysite nanoclay and SiO₂ nanoparticles on barrier and mechanical properties of bovine gelatin films. *Food and Bioprocess Technology*, 5(5), 1766–1774. <https://doi.org/10.1007/s11947-010-0461-y>
- Wang, L., Zheng, D., Zhang, S., Cui, H., & Li, D. (2016). Effect of nano-SiO₂ on the hydration and microstructure of Portland cement. *Nanomaterials*, 6(12). <https://doi.org/10.3390/nano6120241>
- Xu, S.-Y., Huang, X., & Cheong, K.-L. (2017). Recent advances in marine algae polysaccharides: Isolation, structure, and activities. *Marine Drugs*, 15(12). <https://doi.org/10.3390/md15120388>
- Yang, M., Shi, J., & Xia, Y. (2018). Effect of SiO₂, PVA and glycerol concentrations on chemical and mechanical properties of alginate-based films. *International Journal of Biological Macromolecules*, 107, 2686–2694. <https://doi.org/10.1016/j.ijbiomac.2017.10.162>
- Yang, M., & Xia, Y. (2017). Preparation and characterization of nano-SiO₂ reinforced alginate-based nanocomposite films (II). *Journal of Applied Polymer Science*, 134(38), 1–9. <https://doi.org/10.1002/app.45286>
- Yang, M., Xia, Y., Wang, Y., Zhao, X., Xue, Z., Quan, F., ... Zhao, Z. (2016). Preparation and property investigation of crosslinked alginate/silicon dioxide nanocomposite films. *Journal of Applied Polymer Science*, 133(22), 1–9. <https://doi.org/10.1002/app.43489>
- Yerramathi, B. B., Kola, M., Annem Muniraj, B., Aluru, R., Thirumanyam, M., & Zyryanov, G. V. (2021). Structural studies and bioactivity of sodium alginate edible films fabricated through ferulic acid crosslinking mechanism. *Journal of Food Engineering*, 301(October 2020), Article 110566. <https://doi.org/10.1016/j.jfoodeng.2021.110566>